Experimental Demonstration of Non-Foster Self-oscillating Huygens Radiator

L. Vincelj[1], R. W. Ziolkowski[2] and S. Hrabar[1]

[1]University of Zagreb, Faculty of electrical engineering and computing, Unska 3, 10000, Zagreb, Croatia
[2]University of Technology Sydney, 81 Broadway, Ultimo 2007, NSW, Australia
leo.vincelj@fer.hr, richard.ziolkowski@uts.edu.au, silvio.hrabar@fer.hr

***Abstract* – An extension of the basic concept of a self-oscillating non-Foster cross-dipole to a self-oscillating Huygens radiator has been developed theoretically and studied numerically. A proof-of-concept prototype has been built. The realized antenna consists of two orthogonal dipole-loop pairs, a negative impedance converter, and a tuning LC circuit. In this paper we report the basic concepts and the initial results obtained with a scaled RF demonstrator operating in the 60 MHz regime. The preliminary results have demonstrated self-oscillations with nearly-perfect admittance matching over a tuning bandwidth of 1:1.35. The familiar cardioid-like radiation pattern was achieved as designed across the 10% relative bandwidth. These results confirm the efficacy of the basic idea of self-oscillating non-Foster Huygens radiators.**

I. Introduction

A well-known application of negative capacitances and inductances, i.e., the so-called non-Foster elements [1], is to achieve broadband matching of electrically small antennas. The broadband behavior arises from the fact that non-Foster elements possess dispersion properties that are the inverse to those of ordinary (Foster) reactive elements [2]. However, the assurance of stable behavior in practical non-Foster circuits remains a rather challenging issue [3]. An interesting idea that turns instability into a useful feature is the recently reported non-Foster self-oscillating antenna [4]. The original design consisted of two orthogonal dipoles, mutually connected via a negative impedance converter (NIC) and augmented with a tuning LC circuit. The NIC converts the self-admittance of one dipole into its 'negative image', which is then cancelled by the admittance of the second dipole over a theoretically infinite bandwidth. The LC circuit facilitates the selection of a single, but tunable frequency component to attain a nearly perfectly-matched, broadband self-oscillating antenna [4]. Due to the use of orthogonal dipoles, the system in [4] radiates a symmetrical donut-like radiation pattern. This pattern is inconvenient for practical applications, in contrast to the unidirectional Huygens-like systems investigated in the metasurface community [5]. A theoretical and numerical study that merges the concepts of non-Foster self-oscillating antennas [4] with miniaturized planar Huygens antennas [6] was reported recently in [7].

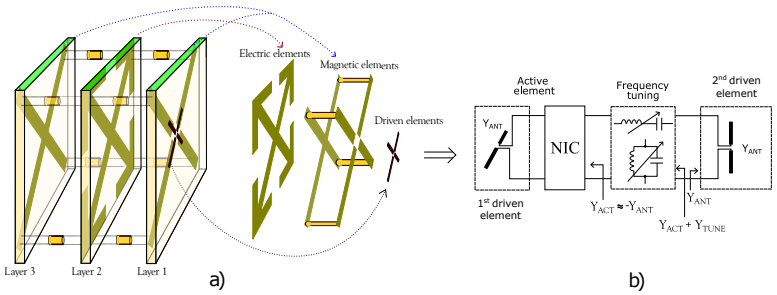

Fig. 1: A self-oscillating non-Foster Huygens radiator. (a) Exploded view. (b) Simplified block diagram.

As Fig. 1 illustrates, the design is again based on a system of two orthogonal 'one-port' antennas, a NIC and a tank circuit. However, in contrast to the original system in [4], each 'one-port' antenna now consists of two separate near-field resonant parasitic (NFRP) element pairs, i.e., a loop and a dipole, each driven by a small dipole.

Both NFRP loop elements are formed by orthogonal traces on Layer 1 and Layer 3 connected by vias passing through Layer 2. Both NFRP dipole elements are formed by orthogonal traces on Layer 2. The fields radiated by the driven dipoles directly induce currents on the NFRP loops. The fields radiated by the NFRP loops have the well-known 'donut' (toroidal) pattern with its nulls in the direction perpendicular to the loop plane, i.e., each NFRP loop acts as a magnetic dipole. The fields they radiate subsequently induce currents on the NFRP elements on Layer 2 which act as electric dipoles. They also radiate toroidal patterns, but with their null directions along the axes of the dipoles. The superpositions of the fields generated by the NFRP dipoles and loops yield the well-known Huygens (cardioid) radiation pattern. The antenna components of the self-oscillating non-Foster Huygens radiator (left part, Fig. 1) designed in [7] were for the 30 MHz RF band. The antenna's footprint was 2.3 m x 2.3 m ($0.23\lambda \times 0.23\lambda$, $ka = 1.02$). This footprint is larger than that of the corresponding passive Huygens radiator developed in [6], 0.11λ x 0.11λ, because the design employed simple styrofoam layers (ϵ_r=1) rather than dielectric ones. The electronic part (right part, Fig. 1) consisted of the floating NIC based on two high-speed THS 4304 operational amplifiers. The EM/circuit simulations predicted stable self-oscillations over a 1:1.5 tuning range and a better than 20 dB suppression of higher harmonics. In this contribution, we refine the design of the electromagnetic (EM) part of the self-oscillating non-Foster antenna developed in [7]. We also describe the manufacturing and testing of an appropriately scaled 60 MHz RF experimental demonstrator and report the preliminary measured results.

II. Non-Foster Self-oscillating Huygens Radiator - Scaled RF Demonstrator

With substantial efforts we discovered that two properties of the initial design [7] could be improved: the return loss and the peak broadside directivity (10 dB and 2.3 dBi, respectively). Further optimization of the geometry of the EM part was performed using various parameter studies with the CST^{TM} software. Once a satisfactory design was obtained, the associated S-matrix was imported into the ADS^{TM} circuit simulator to investigate the self-oscillations. Interestingly, we found that an optimally designed antenna, i.e., the EM design that gives the best return loss and the highest peak broadside directivity, is not necessarily the 'optimal load' for the electronic part. First, the ordinary 50-ohm environment is different from the impedance of the 'equivalent generator' in this case, i.e., the 'negative image' of the second antenna. Second, the antenna's physical dimensions can make a significant difference in the self-oscillating antenna's overall performance. Specifically, the input capacitance/inductance of the antennas are frequency dependent. Therefore, they may be on the same order of magnitude as the NIC parasitics if the antenna is physically small. With CST-ADS co-optimizations, we have redesigned both the antenna and the NIC for operation in a higher RF frequency band (60 MHz). This modification facilitates the optimal trade-off between all of the theoretical and practical system parameters. The new physical dimensions of the EM part are 1m x 1m x 0.09m giving the first resonance at 66.2 MHz. The electric dimensions remained relatively unchanged (0.22λ x 0.22λ x 0.019λ, $ka = 0.98$). We also optimized the NIC gain, which is determined by the feedback resistors (see Fig. 8b in [4]). Samples of the simulated results from the optimized design are shown in Fig. 2. It is clearly seen in Fig. 2a that the cardioid radiation pattern is obtained with a peak broadside directivity of 3.9 dBi. Fig. 2b shows that the simulated tuning range was around 1:2, from 28 to 64 MHz or 78%, with a pronounced negative conversion error of the antenna's conductance. Fig. 2c shows that the maximal imbalance of the power radiated by the HP and VP elements was around 5 dB, while the associated polarization angle imbalance was smaller than 5°. These imperfections are not important since they do not change the net radiated power [4].

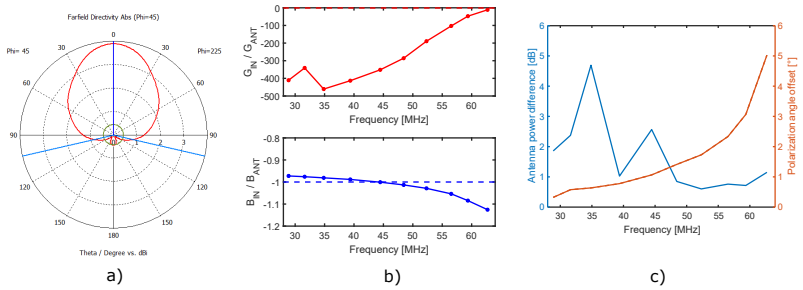

Fig. 2: (a) Simulated radiation pattern of a Huygens antenna (f=66.2 MHz, D=3.9 dBi). (b) Simulated NIC conversion ratio (conductance-upper, susceptance-lower). The ideal cases are depicted dashed, and realistic cases solid. (c) Imbalance in the power radiated by the HP and VP elements (blue) and in their polarization angles (red).

Finally, it is important to notice that the cardioid radiation pattern was obtained over a 10% fractional bandwidth despite the antenna being electrically small, which is significantly narrower than the 78% (1:2) tuning bandwidth. This is a consequence of the fact that 90° phase difference between the induced loop/dipole currents is required to achieve a balanced electric and magnetic dipole pair that generates the Huygens pattern, and it can theoretically be met at only one frequency.

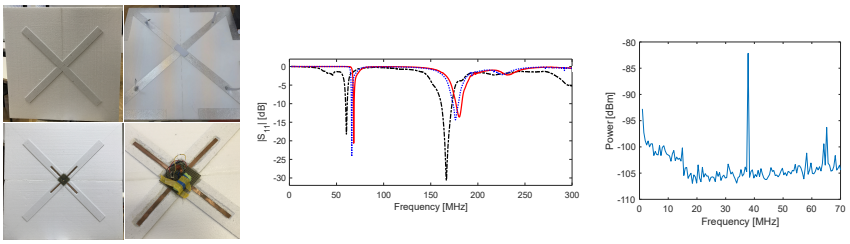

Fig. 3: (a) RF demonstrator. Upper left: Layer 3, top sides of the NFRP loops. Upper right: front side of the NFRP dipoles on Layer 2. Lower left: bottom sides of the NFRP loops on Layer 1. Lower right: electronic parts and the driven dipoles. (b) Comparisons of the $|S_{11}|$ values of the simulated Huygens radiators (solid red and dashed blue) with the measured RF demonstrator (dot dashed black). (c) Measured spectrum of a self-oscillating signal.

The optimized demonstrator was fabricated, assembled and tested (Fig. 3a). The measured resonant frequency was 10% lower than predicted at 60 versus 66.2 MHz (Fig. 3b). Its return loss was slightly worse, but very acceptable at 20 versus 25 dB. Moreover, the measured spectrum of the self-oscillating signal (Fig. 3c) demonstrated 15 dB suppression of any spurious components. The differences between the simulated and measured results are attributed to manufacturing errors. In particular, there was a pronounced discrepancy between the simulated and measured tuning range (28 to 64 MHz, or 1:2, versus 29 to 39 MHz, or 1:1.34). In order to find the reason for this difference, we have simulated different manufacturing errors and misalignments. Observations suggest that variations of the design parameters, which have only a slight influence on the return loss, can have significant impact on the tuning range. While these conclusions are very preliminary, additional investigations of the sensitivity of manufacturing tolerances on the system performance are needed, and are in progress.

III. Conclusion

The concept of a self-oscillating non-Foster Huygens radiator, proposed in a recent numerical study [7], has been investigated further. The design was optimized for a different frequency range and tested experimentally. The measured demonstrator results are consistent with their simulated values, thus verifying the correctness of the idea.

Acknowledgement

The work has been supported by the HRZZ Grant No. IP 2018-01-9753, “Electromagnetic Structures for Emerging Communication Systems”.

References

[1] L. Verman, “Negative circuit constants,” *Proc. Inst. Radio Eng.,* vol. 19, no. 4, pp. 676-681, 1931.
[2] S. Hrabar, “First ten years of active metamaterial structures with ’negative’ elements,” *EPJ Appl. Metamat.,* vol. 5, no. 9, pp. 1-12, 2018.
[3] E. Ugarte-Munoz, S. Hrabar, D. Segovia-Vargas and A. Kiricenko, “Stability of non-Foster reactive elements for use in active metamaterials and antennas,” *IEEE Trans. Antennas Propag.,* vol. 60, no. 7, pp. 3490-3494, 2012.
[4] L. Vincelj, I. Krois and S. Hrabar, “Toward self-oscillating non-Foster unit cell for future active metasurfaces,” *IEEE Trans. Antennas Propag.,* vol. 68, no. 3, pp. 1665-1679, 2019.
[5] H.T. Chen, A.J. Taylor and N. Yu, “A review of metasurfaces: physics and applications,” *Rep. Prog. Phys.,* vol. 79, no. 7, pp. 1-40, 2016.
[6] W. Lin and R.W. Ziolkowski, “Electrically-small, low-profile, Huygens circularly polarized antenna,” *IEEE Trans. Antennas Propag.,* vol. 66, no. 2, pp. 636-643, 2018.
[7] L. Vincelj, S. Hrabar and R.W. Ziolkowski, “Non-Foster self-oscillating Huygens radiator,” Accepted for the *IEEE International Symposium on Antennas and Propagation (APS/URSI),* 2020.